

# Studies of Naphthyl-Substituted $\beta$ -Cyclodextrins. Self-Aggregation and Inclusion of External Guests

Shelli R. McAlpine and Miguel A. Garcia-Garibay\*

Contribution from the Department of Chemistry and Biochemistry, University of California at Los Angeles, Los Angeles, California 90095-1569

Received August 11, 1997

**Abstract:** Studies of 3-*O*-(2-methylnaphthyl)- $\beta$ -cyclodextrin (**1**) with various spectroscopic methods including  $^1\text{H}$  NMR, fluorescence, UV–vis, and circular dichroism yield information on the character of this compound. NOESY data indicate the naphthyl moiety binds inside the cyclodextrin cavity.  $^1\text{H}$  NMR concentration-dependent studies reveal that **1** is a dimer at concentrations of  $>10^{-4}$  M. The circular dichroism spectrum of dilute samples is consistent with a monomer. Analysis of **1** complexing with 2-(*p*-toluidino)-6-naphthalenesulfonate (TNS) with both fluorescence and  $^1\text{H}$  NMR demonstrates that a hydrophobic interaction occurs between **1** and TNS. The concentration dependence of this interaction is strongly affected by the dimerization equilibrium of **1**.

## Introduction

Motivated by developments in host–guest chemistry and improved synthetic methodologies, interest in chromophore-labeled organic receptors such as cyclodextrins,<sup>1–12</sup> crown ethers,<sup>3</sup> and calixarenes<sup>4</sup> has steadily increased over the years. Molecular sensors based on the guest-induced response of fluorescent-labeled cyclodextrins have been developed by several groups. In particular, Ueno *et al.*<sup>6–9,11–27</sup> have demonstrated numerous examples involving cyclodextrins linked

with aromatic hydrocarbons and amino naphthalenesulfonates that are sensitive to their binding state. The sensing capabilities of these compounds depend strongly on the interaction between the guest and the covalently attached probe, and on how their interaction is mediated by the cyclodextrin cavity. Ueno's "induced-fit" complexation is one of the most robust binding-to-fluorescence transduction models where changes in fluorescence signals result from the ability of the guest to change the local environment of a sensitive fluorophore attached to the cyclodextrin (Scheme 1). Examples in Scheme 1 show induced-fit transduction mechanisms that include (a) guest-induced monomer-to-excimer emission in doubly labeled cyclodextrins, (b) guest-promoted binding by space regulation, and (c) displacement of a self-included probe by a hydrophobic guest. Fluorophores that are sensitive to the proximity of another chromophore, to the hydrophilicity of the environment, and to changes in local microviscosity may be adapted to those sensing models. The average location of the probe should change upon binding with a response that depends on a subtle balance between conformational forces and binding interactions.

Because of their relatively large size and complex dynamics, a detailed characterization of cyclodextrin-based molecular sensors and their interactions with guests is challenging. Our own interests center on models where signal transduction is achieved by displacement of a self-included hydrophobic probe by hydrophobic guests (mechanism c in Scheme 1).

To probe the interrelation between conformational aspects, binding interactions and hydrophobic forces, we have selected systems with naphthyl groups acting both as labels (L) and as guests (G) with  $\beta$ -cyclodextrin as the host. In this paper we

(1) Bender, M. L.; Komiyama, M. *Cyclodextrin Chemistry*; Springer-Verlag: Berlin, 1977.

(2) Breslow, R. *Acc. Chem. Res.* **1991**, *24*, 317–324.

(3) Cram, D. J.; Carmack, R. A.; Helgeson, R. C. *J. Am. Chem. Soc.* **1988**, *110*, 571–577.

(4) Shimizu, H.; Iwamoto, K.; Fujimoto, K.; Shinkai, S. *Chem. Lett.* **1991**, 2147–2150.

(5) Hamada, Y.; Kondo, Y.; Ito, R. *J. Inclusion Phenom. Mol. Recognit. Chem.* **1993**, *15*, 273–279.

(6) Hamasaki, K.; Ikeda, H.; Nakamura, A.; Ueno, A.; Toda, F.; Suzuki, I.; Osa, T. *J. Am. Chem. Soc.* **1993**, *115*, 5035–5040.

(7) Hamasaki, K.; Ueno, A.; Toda, F. *J. Chem. Soc., Chem. Commun.* **1993**, 331–333.

(8) Hamasaki, K.; Ueno, A.; Toda, F.; Suzuki, I.; Osa, T. *Bull. Chem. Soc. Jpn.* **1994**, *67*, 7.

(9) Nakamura, M.; Ikeda, A.; Ise, N.; Ikeda, T.; Ikeda, H.; Toda, F.; Ueno, A. *J. Chem. Soc., Chem. Commun.* **1995**, 721–722.

(10) Nakamura, A.; Saitoh, K.; Toda, F. *Chem. Lett.* **1989**, 2209–2212.

(11) Suzuki, I.; Sakurai, Y.; Ohkubo, M.; Ueno, A.; Osa, T. *Chem. Lett.* **1992**, 2005–2008.

(12) Suzuki, I.; Ohkubo, M.; Ueno, A.; Osa, T. *Chem. Lett.* **1992**, 267–272.

(13) Ikeda, H.; Nakamura, M.; Ise, N.; Oguma, N.; Nakamura, A.; Ikeda, T.; Toda, F.; Ueno, A. *J. Am. Chem. Soc.* **1996**, *118*, 10980–10988.

(14) Ikeda, H.; Nakamura, M.; Ise, N.; Toda, F.; Ueno, A. *J. Org. Chem.* **1997**, *62*, 1411–1418.

(15) Kobayashi, N.; Saito, R.; Hino, H.; Hino, Y.; Ueno, A.; Osa, T. *J. Chem. Soc., Perkin Trans. 2* **1983**, 1031–1035.

(16) Ueno, A.; Moriwaki, F.; Osa, T.; Hamada, F.; Murai, K. *Bull. Chem. Soc. Jpn.* **1986**, *59*, 465–470.

(17) Ueno, A.; Moriwaki, F.; Osa, T.; Hamada, F.; Murai, K. *J. Am. Chem. Soc.* **1988**, *110*, 4323–4328.

(18) Ueno, A.; Suzuki, I.; Osa, T. *Chem. Lett.* **1989**, 2013–2016.

(19) Ueno, A.; Suzuki, I.; Osa, T. *J. Am. Chem. Soc.* **1989**, *111*, 6391–6397.

(20) Ueno, A.; Suzuki, I.; Osa, T. *Chem. Lett.* **1989**, 1059–1062.

(21) Ueno, A.; Suzuki, I.; Osa, T. *Anal. Chem.* **1990**, *62*, 2461–2466.

(22) Ueno, A.; Osa, T. *Photochemistry in Organized and Constrained Media*; Ramamurthy, V., Ed.; VCH Publishers: New York, 1991; pp 739–782.

(23) Ueno, A.; Minato, S.; Osa, T. *Anal. Chem.* **1992**, *64*, 2562–2565.

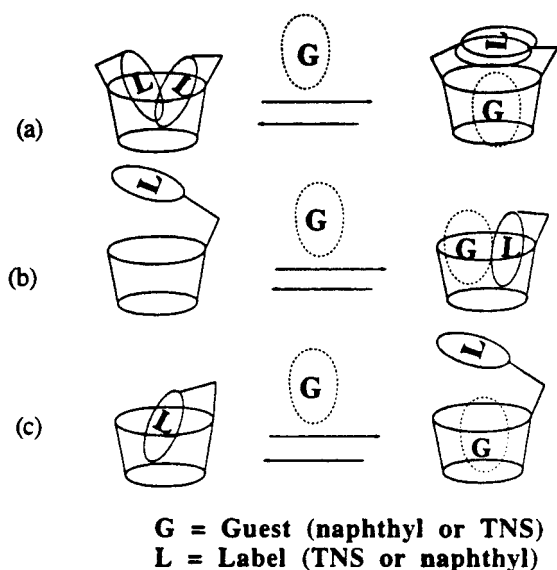
(24) Ueno, A.; Minato, S.; Osa, T. *Anal. Chem.* **1992**, *64*, 1154–1157.

(25) Ueno, A.; Kuwabara, T.; Nakamura, A.; Toda, F. *Nature* **1992**, *356*, 136–137.

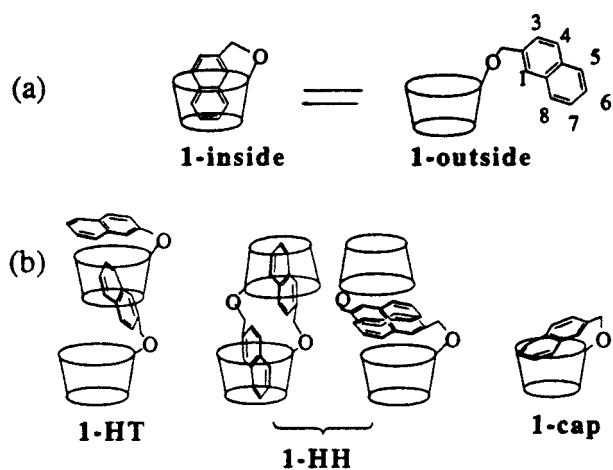
(26) Wang, Y.; Ikeda, T.; Ueno, A.; Toda, F. *Chem. Lett.* **1992**, 863–866.

(27) Wang, Y.; Ikeda, T.; Ikeda, H.; Ueno, A.; Toda, F. *Bull. Chem. Soc. Jpn.* **1994**, *67*, 1598–1607.

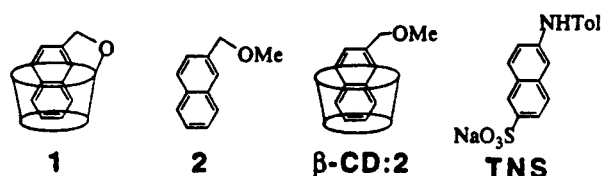
Scheme 1



Scheme 2



Scheme 3



present results with a 3-*O*-(2-methylnaphthyl)- $\beta$ -cyclodextrin as a labeled host (**1**, Scheme 2) and the hydrophobic probe 2-(*p*-toluidino)-6-naphthalenesulfonate (TNS, Scheme 3) as a guest. With a combination of optical spectroscopic techniques that includes fluorescence, fluorescence quenching, and circular dichroism in combination with  $^1\text{H}$  NMR, we have discovered an unusual behavior in the case of compound **1** and TNS. Most significantly, we observed that the binding equilibrium is very slow and complex, as well as highly temperature and concentration dependent. Complex changes in fluorescence are qualitatively paralleled by chemical shifts in the  $^1\text{H}$  NMR spectrum. In a recent communication we interpreted our observations with the 3-*O*-naphthyl compound in terms of a self-included structure (**1-inside**), postulating it to be in conformational equilibrium with a structure where the naphthyl group is excluded (**1-outside**, Scheme 2a).<sup>28</sup> In this paper, we report further spectroscopic studies of **1** that reveal the importance of self-

aggregation to give dimeric structures (**1-HT** and/or **1-HH**, Scheme 2b), as well as to give evidence of a monomer, with a relatively exposed naphthyl group in a cap-like structure (**1-cap**, Scheme 2b). We also analyze the unusual interactions between **1** and TNS in light of fluorescence measurements and  $^1\text{H}$  NMR data. Interactions between the naphthyl moiety of **1** and external guests were first reported with use of fluorescence,<sup>28</sup> and subsequently with use of  $^1\text{H}$  NMR methods.<sup>29</sup> The hydrophobic nature of the postulated monomer is discussed in view of previous and new results.

## Results and Discussion

**Sample Preparation and  $^1\text{H}$  NMR Studies.** As reported in our preliminary communication,<sup>28</sup> compound **1** was obtained pure in 5% yield after HPLC separation of crude obtained from photolysis of 2-naphthyldiazomethane with  $\beta$ -cyclodextrin in  $\text{H}_2\text{O}$ . The reaction presumably occurs via an intermediate carbene-cyclodextrin complex that inserts into a nearby 3-OH group in a photoaffinity labeling-like experiment. Although the reaction is inefficient, our strategy was to bind the naphthyl group as a diazo precursor, expecting the carbene to react inside the cyclodextrin cavity, yielding **1** preferentially to other possible derivatives. The structure of compound **1** was assigned to that of 3-*O*-(2-methylnaphthyl)- $\beta$ -cyclodextrin by comparison of  $^1\text{H}$  NMR data obtained in DMSO with that previously reported by Abelt et al.<sup>30</sup> who first prepared compound **1** in a similar solid-state reaction.

Initial efforts to document the location of the naphthyl group of **1** in  $\text{H}_2\text{O}$  solutions were consistent with the postulated self-included structure of **inside-1** (Scheme 2a). As previously published, spectra measured with ca.  $5 \times 10^{-3}$  M solutions of **1** in  $\text{D}_2\text{O}$  were different from those obtained in  $d_6$ -DMSO.<sup>28</sup> They were also different from the spectra of **2** and the inclusion complex of **2** and  $\beta$ -cyclodextrin ( $\beta$ -CD:2) that serve as models for water exposure and hydrophobic complexation, respectively (Scheme 3). In contrast to the simple aromatic region of **2**, which can be described in terms of  $\alpha$ - and  $\beta$ -naphthyl hydrogens at 7.92–7.82 (4H) and 7.55–7.45 ppm (3H), respectively, the  $^1\text{H}$  NMR spectrum of  $5 \times 10^{-3}$  M **1** in  $\text{D}_2\text{O}$  at ambient temperatures consists of four groups of signals at 7.89 (1H), 7.79 (1H), 7.70 (3H), and 7.38 ppm (2H). Similarities observed between the spectrum of **1** and the spectrum corresponding to the inclusion complex  $\beta$ -CD:2 were also interpreted in terms of a self-included structure for the former. Accordingly, we found NOE enhancements of ca. 2% in the cyclodextrin hydrogens when signals corresponding to the naphthyl group were irradiated at 30 °C. NOESY cross-peaks between aromatic naphthyl signals and  $\beta$ -cyclodextrin (Figure 1) are consistent with inclusion of the naphthyl group as proposed for **inside-1**.

While inclusion of the naphthyl group is unambiguous, the monomeric nature of the postulated structure (**inside-1**) is uncertain. Aggregate structures with the naphthyl group of one molecule included within the cyclodextrin cavity of another may explain the  $^1\text{H}$  NMR data. One such hypothetical structure is represented in Scheme 4. To determine the importance of aggregation equilibria such as that in Scheme 4, we carried out  $^1\text{H}$  NMR measurements over a concentration range between  $2.0 \times 10^{-2}$  and  $1.6 \times 10^{-4}$  M (Figure 2). This concentration range (125-fold) spans the practical limits of NMR detection at the

(28) McAlpine, S. R.; Garcia-Garibay, M. A. *J. Am. Chem. Soc.* **1996**, *118*, 2750–2751.

(29) McAlpine, S. R.; Garcia-Garibay, M. A. *J. Org. Chem.* **1996**, *61*, 8307–8309.

(30) Smith, S. H.; Forrest, S. M.; Williams, D. C.; Cabell, M. F.; Acquavella, M. F.; Abelt, C. J. *Carbohydr. Res.* **1992**, *230*, 289–297.

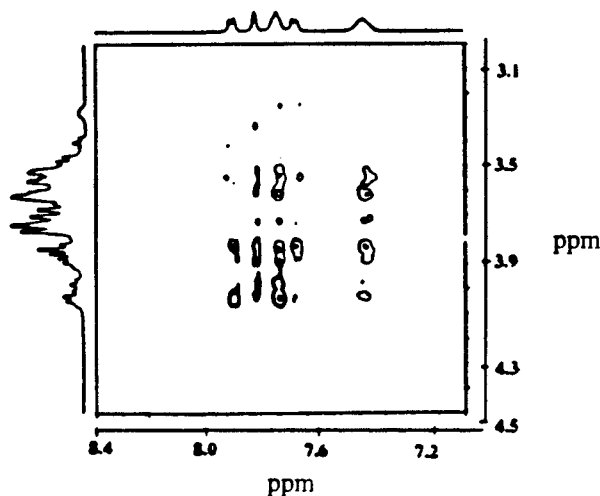
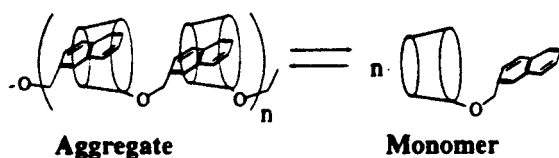


**Figure 1.** 2-Dimensional NOESY  $^1\text{H}$  NMR spectrum of  $10^{-3}$  M **1** in  $\text{D}_2\text{O}$  at  $30^\circ\text{C}$ .

#### Scheme 4



low concentration end to those dictated by the solubility of compound **1** at the high end. The spectrum obtained at  $25^\circ\text{C}$  with concentrated samples ( $2.0 \times 10^{-2}$  M) is similar to those reported before.<sup>28</sup> It is characterized by large upfield shifts of signals assigned to hydrogens inside the cavity (i.e., H5, H6, H7, and H8) with small upfield shifts for H1 (singlet) and H4 (doublet). Successive dilution of the sample resulted in a downfield shift of all but the doublet assigned to H3 (Figure 2b–f). The spectrum of the most dilute sample is characterized by two groups of signals characteristic of the  $\alpha$ - and  $\beta$ -naphthyl hydrogens such as those observed for **2**.

As expected for an aggregation equilibrium that occurs rapidly within the  $^1\text{H}$  NMR time scale, the effect of diluting a concentrated sample is similar to the effect of increasing its temperature. Spectra measured with concentrated samples of **1** ( $2 \times 10^{-2}$  M) at  $50^\circ\text{C}$  qualitatively resemble those of dilute samples (e.g.,  $1.3 \times 10^{-3}$  M) at  $25^\circ\text{C}$ . In a simple equilibrium involving a monomer and a stoichiometrically defined aggregate, these measurements would reflect the populations of all the species involved. However, we noticed that spectra of concentrated samples obtained at high temperatures do not make an exact match with the spectra of dilute samples obtained at low temperatures. This suggests that different types of monomer and/or aggregates may be present at equilibrium at different temperatures.

To evaluate the stoichiometry of the room-temperature aggregate we measured the variation in chemical shifts as a function of concentration (Figure 2).<sup>31</sup> We assumed a dynamic monomer-to-aggregate equilibrium with observed shifts determined by the weighted average of the chemical shifts of the contributing species.<sup>32</sup> The aggregation number,  $n$ , was obtained from the equation:

$$\ln(C_{\text{tot}}\delta_{\text{rel}}) = \ln[C_{\text{tot}}(\delta_{\text{agg}} - \delta_{\text{rel}})] + \ln K + \ln(n) - (n - 1) \ln \delta_{\text{agg}}$$

by plotting  $\ln(C_{\text{tot}}\delta_{\text{rel}})$  against  $\ln[C_{\text{tot}}(\delta_{\text{agg}} - \delta_{\text{rel}})]$  (Figure 3).<sup>31,32</sup>

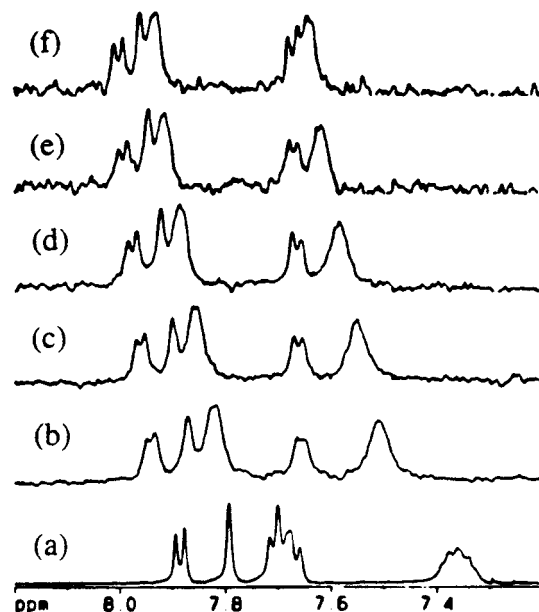


**Figure 2.**  $^1\text{H}$  NMR (500 MHz,  $\text{D}_2\text{O}$ ) spectra of the aromatic region of **1**: (a)  $2.0 \times 10^{-2}$ , (b)  $2.6 \times 10^{-3}$ , (c)  $1.3 \times 10^{-3}$ , (d)  $6.5 \times 10^{-4}$ , (e)  $3.3 \times 10^{-4}$ , and, (f)  $1.6 \times 10^{-4}$  M.

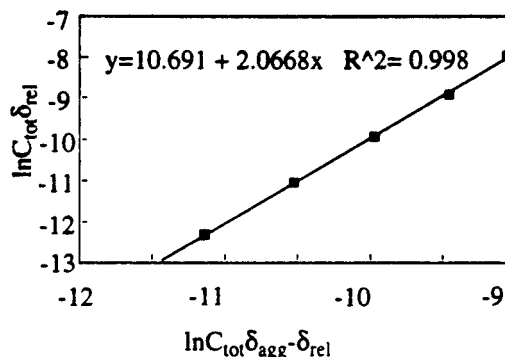


**Figure 3.** Plot from  $^1\text{H}$  NMR data of **1** as a function of total concentration to determine the aggregation number (see text).

The chemical shifts ( $\delta_{\text{obs}}$ ) observed as a function of the total concentration ( $C_{\text{tot}}$ ) were used to calculate the chemical shifts of the monomer ( $\delta_{\text{mon}}$ ) and aggregate ( $\delta_{\text{agg}}$ ). Since dimerization may start at concentrations lower than those observable by  $^1\text{H}$  NMR ( $<10^{-4}$  M) and solubility is poor at concentrations higher than  $10^{-2}$  M, a direct determination of the chemical shifts of the monomer and aggregate in  $\text{D}_2\text{O}$  is not possible. The chemical shift of the monomer was obtained from the intercept of plots of chemical shift versus concentration of **1** as well as from the chemical shift of the dimer from the intercept of plots of chemical shifts as a function of the inverse concentration of **1**. The difference between the  $\delta_{\text{obs}}$  and  $\delta_{\text{mon}}$  yields the value  $\delta_{\text{rel}}$  while  $K$  is the effective equilibrium constant. Differences in extrapolated values for the monomer and dimer (e.g.,  $7.96 \pm 0.01$  ppm and  $7.70 \pm 0.02$  ppm) gave a relatively small uncertainty in the aggregation number ( $n \sim 1.7$ – $2.1$ ). Different aromatic signals also gave relatively narrow aggregation values varying from  $\sim 1.8$  to  $2.1$ , strongly suggesting a dimeric structure. An association constant of *ca.*  $5000 (\pm 500) \text{ M}^{-1}$  at  $25^\circ\text{C}$  can also be determined from the above analysis and a

(31) Seward, E. M.; Hopkins, R. B.; Sauerer, W.; Tam, S.-W.; Diederich, F. *J. Am. Chem. Soc.* **1990**, *112*, 1783–1790.

(32) Menger, F. M.; Whitesell, L. G. *J. Org. Chem.* **1987**, *52*, 3793–3798.

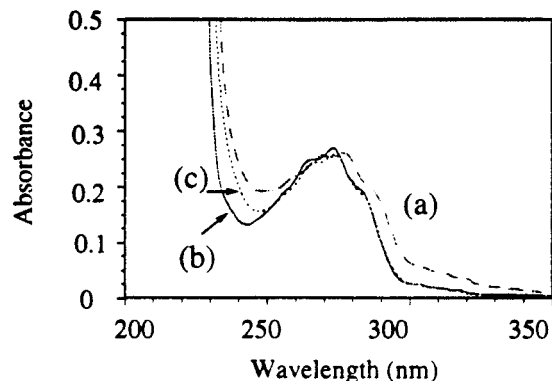


**Figure 4.** (a) UV-vis spectrum of **1**, (b) methyl naphthyl methyl ether (**2**), and (c) the 1:1 complex between  $\beta$ -cyclodextrin and **2** in  $\text{H}_2\text{O}$ .

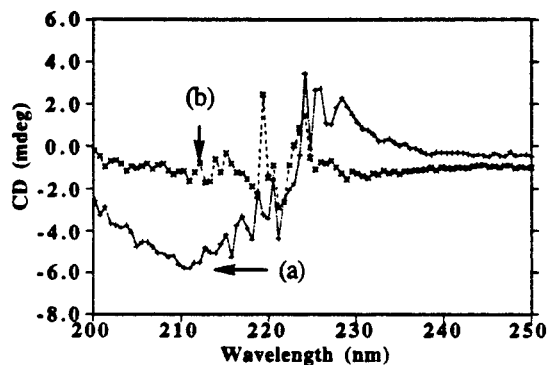


**Figure 5.** (a) Circular dichroism spectrum of  $4.2 \times 10^{-5}$  M aqueous solutions of **1**, and (b)  $4.2 \times 10^{-5}$  M solutions of **2**: $\beta$ -CD at 25 °C.

$\Delta G$  of  $-5.05$  to  $-5.15$  kcal/mol can be calculated from  $K = e^{-\Delta G/RT}$ .

We noted that the free energy value calculated above does not predict correctly the equilibrium populations estimated from  $^1\text{H}$  NMR spectra obtained at higher temperatures. This confirms a complex equilibrium where different monomer and dimer structures are involved at different temperatures. Other complex equilibria with several coexisting species in similar systems have been documented by Wang<sup>27</sup> and Bright.<sup>33</sup> From the  $^1\text{H}$  NMR data obtained at 25 °C, the concentration dependence of **1** is consistent with an aggregation number of two and the NOESY results (taken with **1** at  $1 \times 10^{-3}$  M) dictate a structure with naphthyl groups included within the hydrophobic cavity of cyclodextrin at this concentration. At high concentrations, several dimeric structures may be envisioned that take advantage of inclusion and/or hydrophobic interactions. These can be classified as head-to-head dimers (**HH-1**, Scheme 2b), with the two naphthyl groups in close proximity to each other, and head-to-tail dimers (**HT-1**, Scheme 2b), with only one naphthyl group included. To document whether the structure of the monomer is characterized by self-inclusion, a ROESY spectrum of **1** was measured at  $1 \times 10^{-4}$  M. The lack of cross-peaks in the low concentration ROESY strongly argues against a self-included monomeric structure.

**UV and Circular Dichroism.** The UV-vis spectrum of  $\sim 10^{-5}$  M **1** is slightly red shifted and broadened in comparison to those of naphthylmethyl methyl ether (**2**) and a 1:1 inclusion complex between **2** and  $\beta$ -cyclodextrin with a  $\lambda_{\text{max}}$  at 280 nm (Figure 4). We measured circular dichroism spectra of **1** in  $4.2 \times 10^{-5}$  M solutions (Figure 5), where the monomer is expected to predominate (>95%).

(33) Bright, F. V.; Catena, G. C.; Huang, J. *J. Am. Chem. Soc.* **1990**, *112*, 1343–1346.

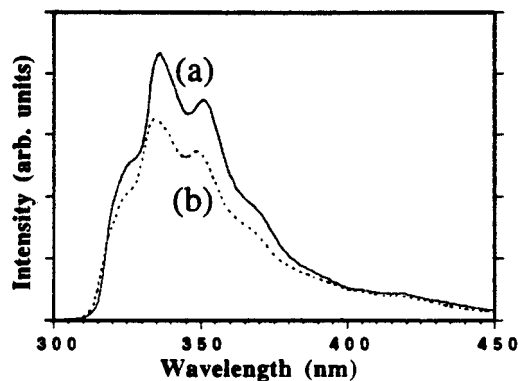


**Figure 6.** Fluorescence emission of (a) compound **1** and (b) the inclusion complex **2**: $\beta$ -CD in  $\text{H}_2\text{O}$  at 25 °C.

Although interpretation must be done with caution, the sign of the circular dichroism (CD) spectrum can be used to define the position of the chromophore.<sup>34</sup> The general rule of Harata and Uedaira<sup>35,36</sup> asserts that a chromophore gives a positive sign when the electronic transitions are polarized along the axes of the cyclodextrin, while a negative sign reveals transitions that are polarized in a perpendicular axis. However, recent refinements by Kodaka<sup>37,38</sup> have shown that the previous rule is only applicable to chromophores bound deep inside the hydrophobic cavity. Partial exclusion decreases the intensity of the signal up to a point where it comes near zero and after which it may even change sign. The  $^1\text{B}_b$  transition in dilute solutions of **1** in  $\text{H}_2\text{O}$  between 200 and 240 nm gave rise to a CD spectrum that changes in sign from negative to positive under conditions where the model inclusion complex gave no observable CD signal (Figure 5). Since the transition dipole moment of the  $^1\text{B}_b$  band is along the long axis of the naphthyl chromophore, inclusion of the naphthyl group with its long axis along the cyclodextrin cavity would give a strong positive CD spectrum. The lack of a strong positive CD signal argues against deeply included structures such as that of **inside-1** which was previously postulated by us. The CD spectrum of compound **1** is in excellent agreement with those observed by Ueno *et al.*,<sup>16</sup> which indicate “cap” structures with the naphthyl group only partially included. This interpretation is also consistent with the lack of cross-peaks in the ROESY spectrum taken at low concentrations of **1**.

**Intrinsic Fluorescence.** Ueno *et al.*<sup>39</sup> have shown that intramolecular excimer fluorescence may be observed from doubly labeled cyclodextrins when a close face-to-face arrangement between the two naphthyl groups may be achieved within the lifetime of the excited state. To investigate the possibility of a similar interaction between two molecules of **1**, a series of fluorescence spectra were obtained in  $\text{H}_2\text{O}$  at concentrations ranging from  $10^{-5}$  to  $10^{-2}$  M and with temperatures ranging between 25 and 85 °C. As shown in Figure 6, dilute ( $10^{-5}$  M) samples gave a broad but structured emission with a  $\lambda_{\text{max}}$  at 335 nm, which is characteristic of a monomeric naphthyl chromophore, with a spectrum nearly identical to that of **2**. Spectra measured as a function of concentration and temperature<sup>40</sup> showed changes in the ratio of intensities at 425 (excimer)

(34) Neckers, D. C.; Volman, D. H.; VonBunau, G. In *Advances in Photochemistry*; John Wiley & Sons: New York, 1996; pp 5–35.

(35) Harata, K.; Uedaira, H. *Bull. Chem. Soc. Jpn.* **1975**, *48*, 375–378.

(36) Harata, K. *Bull. Chem. Soc. Jpn.* **1978**, *51*, 2737–2738.

(37) Kodaka, M. *J. Phys. Chem.* **1991**, *95*, 2110–2112.

(38) Kodaka, M. *J. Am. Chem. Soc.* **1993**, *115*, 3702–3705.

(39) Ueno, A.; Moriwaki, F.; Osa, T.; Hamada, F.; Murai, K. *Tetrahedron* **1987**, *43*, 1571–1578.

(40) Hamai, S. *Bull. Chem. Soc. Jpn.* **1996**, *69*, 543–549.

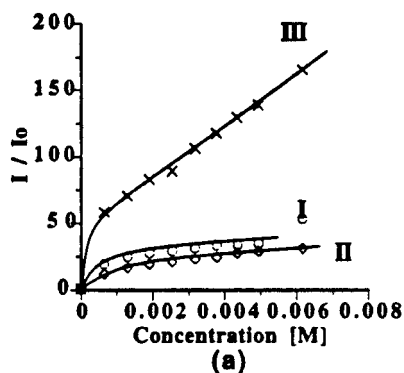


**Figure 7.** Changes in fluorescence intensity of  $10^{-5}$  M TNS to which varying amounts of  $\beta$ -CD (I), complex  $\beta$ -CD:2 (II), and **1** (III) are added (not all data points are shown).

and 335 nm (monomer) smaller than 2%. This indicates that aggregation does not position the two naphthyl groups face-to-face and parallel to each other as required for an excimer. Since it is expected that head-to-head structures **1-HH** should allow for excimer formation, the fact that no such emission was observed suggests either a very restricted mobility with unfavorable arrangement or a structure having one molecule embedded in the cavity of another one as suggested by structures **1-HT** in Scheme 2.

**Fluorescence Studies with TNS.** With the information analyzed above in mind, it is expected that the interaction of **1** with external guests should be complex. It will be mediated by the equilibrium population and dynamics of the monomer and dimer, the concentration of the guest, and their relative affinities to one another. One of the most remarkable observations in our preliminary communication related to the interaction between compound **1** and 2-(*p*-toluidino)-6-naphthalenesulfonate (TNS). We proposed that an inside–outside equilibrium such as that shown in Scheme 2a would affect the inclusion of external TNS as compared to  $\beta$ -cyclodextrin, and we proposed that complexation would be hindered at low temperatures but it would be facile at higher temperatures. Experimental results with TNS over a large range of concentrations of **1** revealed an unexpected behavior that is only partially consistent with such a hypothesis.

We compared changes in fluorescence intensity of TNS as a function of increasing amounts of compound **1** (Figure 7a, line III), an equimolar solution of  $\beta$ -cyclodextrin and **2** (line II), and pure  $\beta$ -cyclodextrin (line I). In agreement with the original report by Kondo,<sup>41</sup> addition of up to ca.  $6 \times 10^{-3}$  M  $\beta$ -cyclodextrin to  $10^{-5}$  M TNS increases the intensity of the latter by a factor of ca. 35 when excitation is carried out at 360 nm and detection at 485 nm (Figure 8a, line I). This increase in fluorescence results from an increase in the hydrophobicity of the environment which destabilizes a nonemissive intramolecular charge-transfer species.<sup>33,41–50</sup> Addition of a 1:1

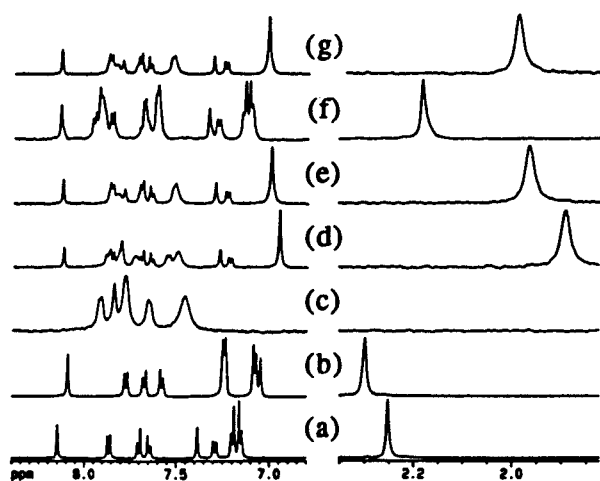


**Figure 8.**  $^1\text{H}$  NMR (500 MHz,  $\text{D}_2\text{O}$ ) spectra of the aromatic and aliphatic regions of TNS ( $2.4 \times 10^{-3}$  M) (a), TNS ( $2.4 \times 10^{-3}$  M) and  $\beta$ -cyclodextrin ( $8.3 \times 10^{-3}$  M) at 25 °C (b), **1** ( $1 \times 10^{-3}$  M) at 25 °C (c), TNS ( $4.5 \times 10^{-4}$  M) and **1** ( $6 \times 10^{-4}$  M) at 25 °C (d), TNS ( $6 \times 10^{-4}$  M) and **1** ( $4.2 \times 10^{-4}$  M) at 25 °C (e), TNS ( $6 \times 10^{-4}$  M) and **1** ( $4.2 \times 10^{-4}$  M) at 25 °C (f), and TNS ( $6 \times 10^{-4}$  M) and **1** ( $4.2 \times 10^{-4}$  M) at 80 °C (g).

complex of **2** in  $\beta$ -cyclodextrin ( $\beta$ -CD:2) gave a similar result (line II). Displacement of line II to lower intensity values results from competitive binding between TNS and **2**, which lowers the concentration of TNS bound. Remarkably, sequential addition of **1** under identical conditions resulted in an overall ca. 165-fold fluorescence increase (line III), indicating an efficient hydrophobic interaction between TNS and **1**, as compared to that between TNS and  $\beta$ -cyclodextrin.

It is known that TNS forms 1:1 and 1:2 complexes with  $\beta$ -cyclodextrin and the behavior observed in line I has been previously analyzed in some detail.<sup>10,41,46,49</sup> In our original model, we expected that a self-included structure (**1-inside**, Scheme 1) would hinder complexation so that TNS would remain in the aqueous medium to give a weak fluorescence intensity. However, the results in Figure 8a indicate that **1** offers TNS an environment that is more hydrophobic than that of  $\beta$ -cyclodextrin itself. Furthermore, changes in the concentrations of **1** lead to unexpected intensity profiles that seem to be far from saturation, even near 0.01 M in **1**. An increase in the concentration of **1** from ca.  $10^{-5}$  to  $10^{-3}$  M, under conditions where the monomer is predominant, leads to a 60-fold increase in TNS emission. A further increase in concentration, in the region where the dimer is anticipated ( $>10^{-3}$  M), leads to comparatively smaller effects. Although the complex nature of the binding of TNS with **1** renders a rigorous fluorometric titration unreliable, the intensity vs concentration profile in Figure 7 agrees qualitatively with the aggregation observed by  $^1\text{H}$  NMR. Greater binding interactions observed at low concentrations correlate with binding of TNS with monomeric **1**, which is expected to have a more available hydrophobic cavity than that of the dimer. Experiments between 25 and 85 °C in  $\text{H}_2\text{O}$  with samples containing **1** and TNS were carried out to probe the effect of thermal annealing. We found that measurements at ambient temperature with freshly prepared samples do not represent equilibrium conditions. The intensity of TNS depends weakly on the concentration of **1** and strongly on whether the sample had been freshly prepared or allowed to stand for a few hours. Samples of **1** and TNS left at ambient temperatures had an initial decrease in TNS intensity which

(41) Kondo, H.; Nakatan, H.; Hiromi, K. *J. Biochem.* **1976**, *79*, 393–405.

(42) Seliskar, C. J.; Brand, L. *J. Am. Chem. Soc.* **1971**, *93*, 5405–5414.

(43) Seliskar, C. J.; Brand, L. *J. Am. Chem. Soc.* **1971**, *93*, 5414–5420.

(44) Catena, G. C.; Bright, F. V. *Anal. Chem.* **1989**, *61*, 905–910.

(45) Crescenci, V.; Gamini, A.; Palleshi, A.; Rizzo, R. *Gazz. Chim. Ital.* **1986**, *116*, 435–440.

(46) Haskard, C. A.; Easton, C. J.; May, B. L.; Lincoln, S. F. *J. Phys. Chem.* **1996**, *100*, 14457–14461.

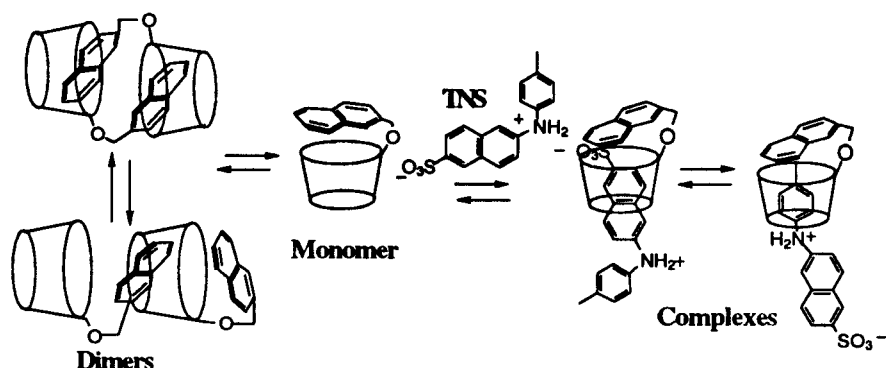
(47) Harada, A.; Furue, M.; Nozakura, S. *Macromolecules* **1977**, *10*, 676–680.

(48) Jobe, D. J.; Verrall, R. E.; Palepu, R.; Reinsborough, V. C. *J. Phys. Chem.* **1988**, *92*, 3582–3585.

(49) Schneider, H.-J.; Blatter, T.; Simova, S. *J. Am. Chem. Soc.* **1991**, *113*, 1996–2000 and references within.

(50) Sarkar, N.; Das, K.; Nath, D.; Bhattacharyya, K. *Chem. Phys. Lett.* **1992**, *196*, 491–495.

## Scheme 5



could be recovered upon heating to 85 °C. Experiments where the temperature was increased to 85 °C in H<sub>2</sub>O and allowed to cool gave the highest intensity values. The results in Figure 7 were obtained at 25 °C with freshly prepared samples and can be reliably reproduced.

**<sup>1</sup>H NMR Studies of **1** and TNS.** To document structural changes occurring when **1** and TNS interact, we carried out a <sup>1</sup>H NMR analysis in D<sub>2</sub>O at different concentrations and at different temperatures. In particular, changes caused by inclusion of the naphthyl and tolyl groups of TNS may be documented in the aromatic region between 6.8 and 8.4 ppm while changes sensed by inclusion of the methyl group of TNS can be observed in the region between 1.9 and 2.4 ppm. The spectrum of pure TNS in D<sub>2</sub>O with samples in the 10<sup>-3</sup> M concentration range is temperature independent (Figure 8a). Schneider *et al.*<sup>49</sup> analyzed the <sup>1</sup>H NMR spectrum of TNS with  $\beta$ -cyclodextrin in D<sub>2</sub>O at 25 °C in terms of dynamic binding involving various 1:1 and 2:1 complexes. On the basis of nanosecond fluorescence spectroscopy, Bright *et al.*<sup>33</sup> proposed that several discrete complexes exist with slightly different geometries. We confirmed that complexation of TNS with  $\beta$ -cyclodextrin at ambient temperatures results in a small upfield shift of all aromatic signals. The spectrum is relatively well resolved with six distinct groups of signals spanning from 8.14 to 7.60 ppm. The methyl group shifts downfield from 2.25 to 2.30 ppm (Figure 8a/8b). Remarkably, addition of **1** at concentrations where the dimer is predominant (Figure 8c) to solutions of TNS to give a 1.0:1.4 ratio (**1**:TNS) results in signal broadening and uneven shifting. While the aromatic signals of TNS shift upfield (relative to those in pure D<sub>2</sub>O), the naphthyl signals of **1** displace downfield. The upfield shift of TNS suggests inclusion in the cavity **1** and the downfield shift of the signals of the naphthyl group of **1** is similar to that recently observed upon displacement by adamantane carboxylic acid.<sup>29</sup> These shifts suggest that TNS interacts with the dimer to displace the naphthyl group from the cavity to form a 1:1 TNS:**1** inclusion complex (Figure 8d).<sup>28,29</sup> The region between 1.9 and 2.5 ppm gives further insight into the structural changes occurring when TNS interacts with **1**. As a reference, a 0.05 ppm downfield shift of the methyl signal of TNS upon addition of  $\beta$ -cyclodextrin is consistent with a time-average inclusion of the tolyl group and is thought to be caused by its close proximity with the cyclodextrin inner glycosidic oxygens.<sup>49</sup> This shift is similar to that seen for 1-adamantane carboxylic acid bound to  $\beta$ -cyclodextrin.<sup>29</sup> In contrast, addition of TNS to **1** in a 1.4:1.0 ratio shifts the methyl peak upfield to 1.89 ppm, indicating a time-average environment where the methyl group is now influenced by the diamagnetic shielding caused by the proximity of the naphthyl group of **1**.<sup>29</sup> Upon heating to 80 °C, a downfield shift of the aromatic signals and the methyl

group indicates that the equilibrium is displaced toward the dissociated species (Figure 8f). Although the final shifts of the TNS aryl and methyl signals were dependent on the ratio of TNS to **1**, the final chemical shifts of the naphthyl group of **1** were not significantly different regardless of its initial concentration. This is presumably because TNS binds to the monomer of **1**.

An interpretation of Figure 8 based on inclusion-induced chemical shift changes requires the participation of several species and is qualitatively consistent with an equilibrium such as that depicted in Scheme 5. In analogy to the 1:2 binding modes of  $\beta$ -cyclodextrin and TNS, one may postulate that TNS binds to **1** with a 1:1 stoichiometry to maintain a hydrophobic interaction with the naphthyl moieties of **1** and TNS. The formation of 2:1 TNS:**1** complexes is also unlikely because the naphthyl group of **1** is expected to hinder entry through the secondary side of the cyclodextrin cavity.

## Conclusions

The concentration dependence of the <sup>1</sup>H NMR of compound **1** reveals a highly dynamic monomer–dimer equilibrium with structures possessing one or two naphthyl groups in their hydrophobic cavities. Circular dichroism obtained at high dilution suggests monomers with a cap-like structure rather than a deeply included naphthyl group. Fluorescence measurements show no indication of excimer emission, thus indicating either head-to-head dimers **1-HH** in conformations unable to form the expected face-to-face arrangement or head-to-tail dimer **1-HT** where only one naphthyl group is included. Fluorescence measurements with dilute solutions of **1** and 2-(*p*-toluidino)-6-naphthalenesulfonate (TNS) reflect the complexity of the interactions that occur between the monomer, dimer, and hydrophobic guest. The <sup>1</sup>H NMR data of **1** and TNS at 10<sup>-3</sup> M concentrations confirm the hydrophobic interactions observed with fluorescence, and suggest a 1:1 complex between TNS and **1**. The NMR results are consistent with the effects observed previously with **1** and adamantane carboxylic acid<sup>29</sup> and the dimer–monomer model proposed, where the dimer equilibrium is disrupted upon guest binding. The structure and properties of **1** that emerge from a combination of spectral techniques demonstrate a significant temperature and concentration dependence of **1**. These studies reflect the high degree of complexity in this system, especially when guest binding is involved. The results reported above may help develop a model that can be applied to similar systems and may lead to a better understanding of chemical sensors based on host–guest interactions.

## Experimental Section

**General.** All Solvents used were the highest purity commercially available and were used as received.  $\beta$ -Cyclodextrin was generously

donated by American Maize Products and was used as received. 3-O-(2-methylnaphthyl)- $\beta$ -Cyclodextrin (**1**) was prepared as described in the literature.<sup>28,29</sup> (2-naphthyl) methyl-methyl ether was prepared from 2-naphthylaldehyde (Aldrich) by standard procedures. Inclusion complexes for <sup>1</sup>H NMR studies were prepared by dissolving known amounts of guest and host in D<sub>2</sub>O. Separations and purifications were carried out on a Waters 600E HPLC with a photodiode array detector and a C18  $\mu$  Bondapak column of 3.9 mm by 300 mm. The circular dichroism was taken on an Aviv instrument model 62 ADS.

**Variable-Temperature NMR.** <sup>1</sup>H NMR spectra were obtained in a Bruker 500 MHz ARX NMR instrument with a 5 mm inverse broad band probe. Measurements were taken after spinning the sample in the probe at least 10 min at each selected temperature. The instrument was only shimmed at 298 K but the probe was tuned at every temperature before the spectra were taken. Thirty-two scans with a 30° excitation pulse were accumulated at each temperature. Chemical shifts were measured relative to external acetic anhydride (=3.08 ppm) as well as internal comparisons with use of the anomeric protons. Residual protons in D<sub>2</sub>O shifted from 4.70 ppm at 298 K to 4.40 ppm

at 323 K and 4.10 ppm at 353 K. The host-to-guest ratio was confirmed by integration of the anomeric hydrogens relative to the signals of the guest.

**Fluorescence Measurements.** Fluorescence spectra were recorded with a Spex-Fluorolog instrument equipped with a thermostated sample holder. Quenching experiments were carried out by addition of 0.5 M potassium iodide in total amounts of 1, 10, 20, 40, 100, 150, and 200  $\mu$ L amounts. Optical densities of 0.1 were measured with a UV-vis Beckman DU-600 instrument before measuring the fluorescence intensity with an excitation wavelength of 275 nm and emission at 333 nm.

**Acknowledgment.** We acknowledge support by the National Science Foundation and the NIH for a Chemistry and Biochemistry Interface Training Grant to S.R.M. (NIH-GM08496). We also thank Dr. J. M. Strouse for help with NMR measurements.

JA972810P